

Scattering Properties of a Model Bicontinuous Structure with a Well Defined Length Scale

N. F. Berk

Institute for Materials Science and Engineering, National Bureau of Standards, Gaithersburg, Maryland 20899
(Received 10 October 1986)

Cahn's scheme for simulating the morphology of isotropic spinodal decomposition is adapted to a mathematical model of bicontinuous partitioning of space by interfacial pairs that may be useful for problems of microdispersed and microporous systems distinguished by a morphology with a well defined length scale, including surfactant films in microemulsions and coatings in porous media. Real-space and scattering properties are analyzed, and qualitatively the model accounts for the principal features of recent contrast-variation small-angle neutron-scattering experiments on Winsor III type microemulsions.

PACS numbers: 82.70.Kj, 61.12.Bt, 61.90.+d

Contrast-variation small-angle neutron-scattering experiments¹⁻³ indicate that microemulsions of the Winsor III type containing equal volumes of oil and water are bicontinuous structures in the sense that the subvolumes occupied by oil and water, while densely interspersed, are each physically connected across the specimen, possibly as the fluid analog of porous solids.⁴ [Microemulsions are oil and water mixtures stabilized by surfactant. Winsor III type coexist with excess oil and water; I (II), with excess oil (water).] Evidence for this morphology comes from measurements in which scattering from the interfacial surfactant medium is enhanced by matching of the scattering-length densities of oil and water to eliminate the contrast between them. The featureless intensity observed at this contrast by de Geyer and Tabyony^{1,2} decreases monotonically with increasing wave vector and cannot be interpreted in terms of closed spherical shells of surfactant mixture, as can the scattering observed for microemulsions sufficiently far removed from oil and water isometry (Winsor I and II)^{1,2} and for microemulsions in which bicontinuous structure is inhibited by spontaneous curvature of the surfactant film, which favors globules.⁵ Furthermore, determination¹ of the Patterson function shows that in the Winsor III phase the surfactant film extends continuously over distances large compared with physically reasonable droplet sizes,¹ and cross-correlation measurements by Auvray *et al.*³ indicate that this interfacial film has zero mean curvature, implying a disordered bicontinuous structure.³ However, when the dominant contrast is between oil and water, a prominent peak is observed,¹ which is inconsistent with existing models of randomly interpenetrating two-phase microstructures,⁶ including those based on Voronoi tessellation.⁷ This peak may thus indicate a structure with a definite length scale, and recent theories⁸⁻¹¹ suggest that a key feature of Winsor III microemulsions is that they have a well defined length scale imposed by the bending rigidity of the surfactant layer.^{8,9,11} We show here that an algorithm originally invented by Cahn¹² to simulate morphology influenced by spinodal decomposition in isotropic two-phase systems

—where a well defined length scale also emerges—can be adapted to the description of the scattering properties of these microemulsions.

Cahn's scheme¹² associates an interface between two material phases of uniform density with a level set (contour) of a random standing wave, $S_N(\mathbf{r})$, composed of N sinusoids having *fixed wavelength* λ , but random directions $\hat{\mathbf{k}}_n$, phase constants ϕ_n , and amplitudes A_n :

$$S_N(\mathbf{r}) = \frac{1}{(N\langle A^2 \rangle)^{1/2}} \sum_{n=1}^N A_n \cos(k \hat{\mathbf{k}}_n \cdot \mathbf{r} + \phi_n), \quad (1)$$

where $k = 2\pi/\lambda$ and $\langle A^2 \rangle$ is the mean square sinusoid amplitude. The normalization is chosen here so that the rms wave amplitude is of order unity. For example, for an isometric partition, a two-phase interface coincides with the zero set of $S_N(\mathbf{r})$ —the set $\{\mathbf{r}\}$ on which $S_N(\mathbf{r}) = 0$ —since over a large space (1) is positive as often as it is negative. Cahn's numerical simulations of this process are remarkably evocative of the morphology of phase-separated glasses, as imaged by micrographic techniques; the model structure is highly interconnected, even well away from volume-fraction isometry.¹²

We extend this approach to a description of the interspace between a pair of interfaces associated with two nearby level sets of the same wave, say the α set and the β set [such that $S_N(\mathbf{r}) = \alpha$ and β], to provide a new model for an interfacial film or coating, while the two regions contiguous to this define the complementary bulk partitions appropriate to the problem. For example, see Figs. 1 and 2.

Thus for the wave (1) we define the leveled density field of the (α, β) interspace by

$$\rho(\mathbf{r}) = \theta_{\alpha\beta}(S_N(\mathbf{r})), \quad (2)$$

where $\theta_{\alpha\beta}(S) = 1$ for $\alpha \leq S \leq \beta$, 0 otherwise. The density self-correlation function, $\Gamma(r) = \langle \rho(\mathbf{r})\rho(\mathbf{0}) \rangle$, where angular brackets denote an ensemble average over the random parameter space, can then be exactly expressed as

Work of the U. S. Government
Not subject to U. S. copyright



FIG. 1. White marks the $(-0.14, 0.14)$ interface of (1) for $N=50$ and $A_n=1$, sampled in a planar section.

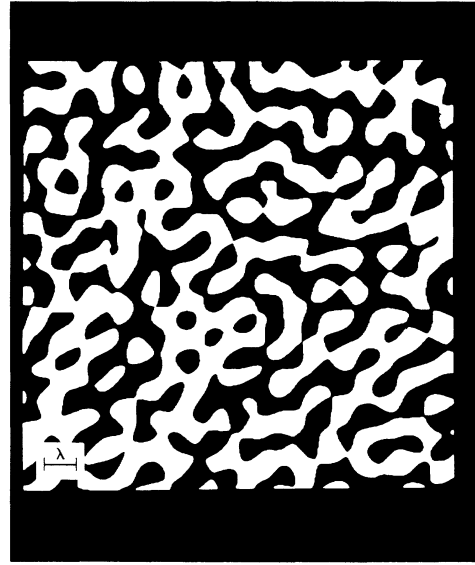


FIG. 2. White-black interface is the zero set of the same standing wave used in Fig. 1.

the double integral

$$\Gamma(r) = \frac{\delta^2}{\pi^2} \int \int_{-\infty}^{\infty} dx dy j_0(\delta x) j_0(\delta y) e^{2i\epsilon(x+y) - g(x,y;r)}, \tag{3}$$

where $\delta = \beta - \alpha$, $\epsilon = (\alpha + \beta)/2$, $j_0(x)$ is the spherical Bessel function, and

$$g(x,y;r) = - \sum_{m=1}^{\infty} \frac{(-1)^m \kappa_{2m}(x,y;r)}{N^{m-1} \langle A^2 \rangle^m (2m)!}. \tag{4}$$

$\kappa_n(x,y;r)$ is the n th cumulant¹³ average of $2A[x \cos(kr\mu + \phi) + y \cos(\phi)]$ over independently distributed A , μ , and ϕ . Only even cumulants contribute since ϕ is uniform over $(0, 2\pi)$; also, μ is uniform over $(-1, 1)$, corresponding to a uniform distribution of \mathbf{k} on the unit sphere. The $m=1$ term is independent of N , and thus is the important one as N becomes large, in keeping with Cahn's observation that the simulated morphology stabilizes rapidly with increasing N .¹² The limit of $\Gamma(r)$ as $N \rightarrow \infty$ thus is representative of the large- N behavior of the leveled wave morphology—to which we now specialize—and is obtained from (3) with

$$g(x,y;r) = x^2 + y^2 + 2xy j_0(kr). \tag{5}$$

The spherical Bessel function in (5) is the self-correlation of the random sinusoid $\sqrt{2} \cos(\mathbf{k} \cdot \mathbf{r} + \phi)$. $\Gamma(r)$ is independent of the A distribution in the infinite- N limit. With (5) in (3) one verifies that $\Gamma(\infty) = \Gamma(0)^2$ and $c_0 = \Gamma(0) = [\text{erf}(\beta) - \text{erf}(\alpha)]/2$, where c_0 is the volume fraction occupied by the interspace and $\text{erf}(x)$ is the error function. The bulk partitions have volume fractions $c_1 = [1 - \text{erf}(\beta)]/2$ and $c_2 = [1 + \text{erf}(\alpha)]/2$, with $c_0 + c_1 + c_2 = 1$. Cahn's two-phase model is retrieved by our

taking $\alpha \rightarrow -\infty$. The leading behavior of $\Gamma(r)$ near $r=0$ is found to be $\gamma(r) \sim 1 - r/\xi$, where $\gamma(r) = [\Gamma(r) - c_0^2]/c_0(1 - c_0)$ is the fluctuation self-correlation of the interspace, with $\gamma(0) = 1$ and $\gamma(\infty) = 0$, and where

$$\xi = c_0(1 - c_0) \sqrt{3} \lambda / (e^{-\beta^2} + e^{-\alpha^2}) \tag{6}$$

can be identified with the mean chord length.¹⁴ The linearity of $\gamma(r)$ at the origin is distinctive of sharp, smooth boundaries. The total interfacial area Σ contained in sample volume V is thus defined for the leveled wave model by the use of (6) in Porod's formula, $\xi = 4c_0(1 - c_0)V/\Sigma$.¹⁴ For the special case of isometric two-phase morphology ($\alpha \rightarrow -\infty, \beta = 0$) the integral in (3) can be completely reduced, leading to

$$\gamma(r) = (2/\pi) \arcsin[j_0(kr)]. \tag{7}$$

This gives $\xi = \sqrt{3}\lambda/4$, in agreement with (6). For $r \rightarrow \infty$, $\gamma(r) \sim 2j_0(kr)/\pi$, which is characteristic of the *unleveled* wave (1), and explains for the first time the appearance of a sharp diffraction peak from the two-phase model as observed in optical Fourier transforms.¹⁵

The intensity of scattered radiation from the interspace in Born approximation is

$$J(q) = c_0(1 - c_0) \int_0^{\infty} r^2 \gamma(r) j_0(qr) dr \tag{8}$$

multiplied by $4\pi V \eta^2$, where q is the scattering wave vector, and η is the contrast between the interspace medium

and matched bulk partitions. Expanding $\exp(-g)$ in (3) and using (5) leads to a uniformly convergent series representation,

$$c_0(1-c_0)\gamma(r) = \sum_n C_n j_0^n(kr),$$

which may be integrated term by term in (8). The C_n are

$$C_n = \frac{1}{\pi n! 2^n} [e^{-\beta^2} H_{n-1}(\beta) - e^{-\alpha^2} H_{n-1}(\alpha)]^2 \quad (9)$$

for $n=1, \dots$; $H_n(x)$ is the Hermite polynomial. Thus, for $N \rightarrow \infty$,

$$J(q) = \frac{\pi}{2k^2} C_1 \delta(q-k) + \frac{\pi}{4qk^2} C_2 \theta_{0\infty}(2k-q) \quad (10)$$

plus a nonsingular remainder encompassing the contribution starting with the $n=3$ term, which I do not discuss here. The first term in (10), the transform of $j_0(kr)$, describes a sharp diffraction line at $q=k$, while the second, the transform of $j_0^2(kr)$, diverges hyperbolically as

$q \rightarrow 0$. As mentioned at (7), the line is associated with the unleveled wave underlying the morphology and is not broadened by the Fourier components introduced implicitly by leveling. The hyperbolic divergence is totally absent from the isometric two-phase case described by (7), which generates an odd $j_0(kr)$ series, while for small c_0 and $\Delta c = c_2 - c_1$, $C_1 \approx 128c_0^2(\Delta c)^2/\pi^3$ and $C_2 \approx 8c_0^2/\pi^2$, showing that the diffraction peak is extinguished rapidly as $\Delta c \rightarrow 0$, where only even powers of $j_0(kr)$ contribute. Thus, at isometry $1/q$ is the only scattering singularity from the interfacial film, a novel diffraction effect associated with the algebraic decay of correlations in the topology.

In practice it is more realistic to introduce some k dispersion into the modes generating the structure. If the wave numbers of the sinusoidal population in (1) have probability density $P(k)$, then $j_0(kr)$ in (5) is replaced by $\tau(r) = \int P(k) j_0(kr) dk$. Taking $P(k)$ as a narrow Gaussian, centered on k_0 with variance Δk^2 , gives $\tau(r) \approx j_0(kr) \exp(-\Delta k^2 r^2/2)$, and the two terms shown in (10) are consequently replaced by

$$J(q) = \frac{(\pi/2)^{1/2} C_1}{2k_0 q \Delta k} \left[\exp\left[-\frac{(q-k_0)^2}{2\Delta k^2}\right] - \exp\left[-\frac{(q+k_0)^2}{2\Delta k^2}\right] \right] + \frac{\pi C_2}{8k_0^2 q} \left[2 \operatorname{erf}\left[\frac{q}{2\Delta k}\right] - \operatorname{erf}\left[\frac{q-2k_0}{2\Delta k}\right] - \operatorname{erf}\left[\frac{q+2k_0}{2\Delta k}\right] \right]. \quad (11)$$

The line is broadened, while the hyperbolic divergence is moderated to $1/\Delta k$ at the origin. Equation (11) is shown in Figs. 3 and 4 for the two limiting contrasts employed in neutron-scattering measurements on Winsor III microemulsions,^{1,2} c_1 standing for either oil or water. Figure 3 represents contrast between oil and water phases only (take $\alpha \rightarrow -\infty$ and redefine c_0 and c_2 in an evident way) while Fig. 4 corresponds to contrast between the surfactant interspace and the matched oil and

water bulk. The general behavior near bulk isometry is similar in both cases to the observed scattering^{1,2} and shows how the peak at one contrast and the monotonic decrease at the other can both be reconciled with a disordered bicontinuous structure.

The leveled wave method thus provides the first unified

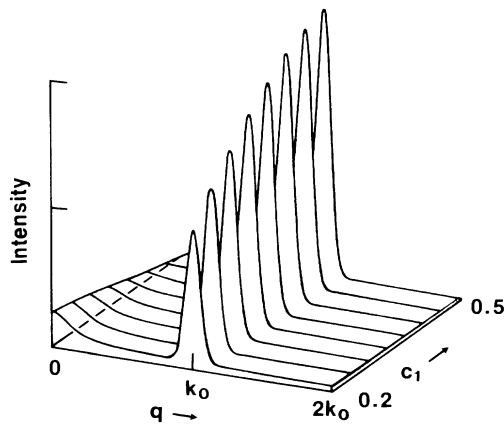


FIG. 3. Scattering intensity for oil-water contrast (single interface); Eq. (11), normalized to the maximum, for $c_0=0$, $\Delta k/k_0=0.05$, and a range of c_1 .

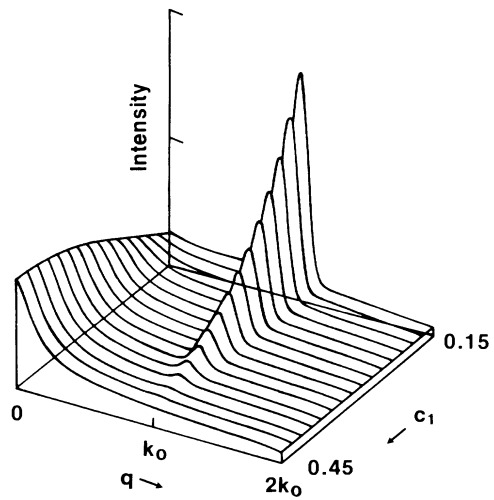


FIG. 4. Scattering intensity for surfactant-bulk contrast (double interface); Eq. (11), normalized to the maximum, for $c_0=0.1$, $\Delta k/k_0=0.05$, and a range of c_1 .

description of the main features of contrast-variation scattering data from the Winsor III phase, reinforcing the idea that these microemulsions, although disordered, have a morphology with a definite length scale—fixed in the model by the common wavelength of the modes used to construct the random sum in (1). The nonequilibrium processes responsible for mode selection in spinodal decomposition are different from the equilibrium competitions that stabilize Winsor III microemulsions, but such physically distinct systems may have related topological properties stemming from the imposition of a well defined length scale.

The character of Cahn's morphology is further elucidated by its curvature properties. If κ_1 and κ_2 are the local principal curvatures¹⁶ on a β set, the local mean curvature, $H = (\kappa_1 + \kappa_2)/2$, may be computed from $H = \nabla \cdot \hat{\mathbf{n}}/2$, where $\hat{\mathbf{n}}(\mathbf{r})$ is the unit normal vector field generated by $S(\mathbf{r}) = -S_N(\mathbf{r})$ of (1). Then, on a β set $H(\mathbf{r}) = [k^2\beta + S''(\mathbf{r})]/2S'(\mathbf{r})$, where the prime denotes the normal derivative. For $N=50$, numerical simulation gives $\langle H \rangle \approx 0.7k\beta$, where $\langle x \rangle = \int x d\Sigma/\Sigma$ here denotes the average over the surface Σ , so that $\langle H \rangle = 0$ on a zero set, the surface separating isometric bulk partitions, consistent with Auvray *et al.*³ For a family of parallel surfaces [constant $S'(\mathbf{r})$], the local Gauss curvature, $K = \kappa_1\kappa_2$, satisfies $K(\mathbf{r}) = 2H(\mathbf{r})^2 - |H'(\mathbf{r})|^2$.¹⁷ With $S' = D$, one then has $H = k^2\beta/2D$ and $K = k^4(\beta^2 - D^2/k^2)/2D^2$; for $\beta=0$, in particular, $H=0$ and $K = -k^2/2$, independent of D . Such a surface is saddlelike everywhere and satisfies formal requirements for nonplanar minimum area.¹⁶ The actual β sets of (1) are not a parallel family—the film in Fig. 1 is not uniform—but on the average the zero set has qualities of a minimal surface, with simulations giving $D \approx \langle S' \rangle = k/\sqrt{2}$ and $\langle H^2 \rangle \approx 0.04k^2$, so that $\langle K \rangle \approx -k^2/2$. These properties (near the zero set) confirm Scriven's conjecture¹⁸ on the minimal property of Cahn's isometric morphology and are consistent with physical interfaces having very small spontaneous curvature, as required for a description of Winsor III microemulsions.¹¹ Finally, for isometric bulk partitions, the interspace described here has average thickness $d \approx 2\beta/D = 0.4c_0\lambda$. Thus, taking $\lambda = 48$ nm

from the position of the peak in the Winsor III scattering at oil-water contrast² and $c_0 = 6\%$,^{2,3} assuming that all the surfactant-cosurfactant mixture resides in the film, we get $d = 1.1$ nm, in agreement with the reported thickness estimate ($d \approx 1$ nm).^{3b}

The author is grateful to C. J. Glinka for invaluable discussions about this work.

¹A. de Geyer and J. Tabony, *Chem. Phys. Lett.* **124**, 357 (1986).

²A. de Geyer and J. Tabony, *Chem. Phys. Lett.* **113**, 83 (1985).

^{3a}L. Auvray, J. P. Cotton, R. Ober, and C. Taupin, *J. Phys. Chem.* **88**, 4586 (1984).

^{3b}L. Auvray, J. P. Cotton, R. Ober, and C. Taupin, *Physica (Amsterdam)* **136B**, 281 (1986).

⁴L. E. Scriven, *Nature (London)* **263**, 123 (1976).

⁵M. Kotlarchyk, S. H. Chen, J. S. Huang, and M. W. Kim, *Phys. Rev. Lett.* **53**, 941 (1984).

⁶P. Debye, H. R. Anderson, and H. Brumberger, *J. Appl. Phys.* **28**, 679 (1957); S. Torquato and G. Stell, *J. Chem. Phys.* **80**, 878 (1984).

⁷E. W. Kaler and S. Prager, *J. Colloid Interface Sci.* **26**, 359 (1982).

⁸P. G. de Gennes and C. Taupin, *J. Phys. Chem.* **86**, 2294 (1982).

⁹J. Jouffroy, P. Levinson, and P. G. de Gennes, *J. Phys. (Paris)* **43**, 1241 (1982).

¹⁰B. Widom, *J. Chem. Phys.* **81**, 1030 (1984).

¹¹S. A. Safran, D. Roux, M. E. Cates, and D. Andelman, *Phys. Rev. Lett.* **57**, 491 (1986).

¹²J. W. Cahn, *J. Chem. Phys.* **42**, 93 (1965).

¹³R. Kubo, *J. Phys. Soc. Jpn.* **17**, 1100 (1962).

¹⁴G. Porod, in *Small Angle X-Ray Scattering*, edited by O. Glatter and O. Kratky (Academic, New York, 1982).

¹⁵J. Zarzycki and F. Naudin, *J. Non-Cryst. Solids* **1**, 215 (1969).

¹⁶T. Y. Thomas, *Concepts from Tensor Analysis and Differential Geometry* (Academic, New York, 1961).

¹⁷This formula follows from Ref. 16, Chap. 24

¹⁸L. E. Scriven, in *Micellization, Solubilization, and Microemulsions*, edited by K. L. Mittal (Plenum, New York, 1976), Vol. 2, p. 877.